EPJ manuscript No.
(will be inserted by the editor)

Tilt angle of lipid acyl chains in unilamellar vesicles determined by ellipsometric light scattering

Andreas Erbe[a] and Reinhard Sigel[b]

Max Planck Institute of Colloids and Interfaces, Wissenschaftspark Golm, Am Mühlenberg 1, 14476 Golm, Germany

Received: date / Revised version: date

Abstract. Ellipsometric light scattering (ELS) at room temperature is applied to unilamellar vesicles (∼50 nm radius) of 1,2-Dipalmitoyl-*sn*-glycero-3-phosphocholine (DPPC) in the gel phase and of 1,2-Dioleoyl-*sn*-glycero-3-phosphocholine (DOPC) in the liquid–crystaline phase. A high sensitivity of this technique to the local anisotropy is found. From the resulting local birefringence, a lower limit of $(29 \pm 0.5)^\circ$ for the average tilt angle of the lipid chains of DPPC with respect to the membrane normal is estimated. This tilt angle value is slightly lower than literature values for the tilt angle in oriented lipid multi-bilayers on solid substrates.

PACS. 87.16.Dg membranes, bilayers, and vesicles – 42.68.Mj scattering, polarization – 42.81.Gs birefringence, polarization

1 Introduction

Lipid vesicles, solid-supported planar lipid bilayers and phospholipid monolayers serve as excellent model systems for the walls of biological cells, which is reflected in the vast amount of research literature in the respective field [1–5]. For the study of membrane proteins, mimicking a native-like biological membrane with enough free space on both sides of the lipid bilayer is of crucial importance [6–9]. From this point of view, vesicles are seen as closest to the actual cell wall. They are embedded into a bulk medium, as opposed to planar mono- and bilayers, where the presence of an interface always restricts incorporated membrane constituents. The planar geometry of the latter two model systems enables, however, their much more detailed study with highly sophisticated physical-chemical characterization methods, e. g. a variety of opti-

[a] *Present address:* Academia Sinica, Institute of Physics, 128 Academia Road Sec. 2, Nankang, Taipei, 11529, Taiwan, e-mail: aerbe@arcor.de

[b] e-mail: sigel@mpikg.mpg.de

cal surface spectroscopy techniques, X-ray and neutron scattering and reflectivity measurements, nonlinear optical techniques, electrical measurements, scanning force microscopy, quartz crystal microbalance studies, to name only a view [9–13]. For dispersed vesicles on the other hand, one is limited with a few exceptions to transmission spectroscopies and scattering methods [8,14].

One crucial detail for the understanding of the structure of lipid monolayers and bilayers at interfaces is the average tilt angle β of the lipid chains with respect to the surface normal [15–20]. The determination of β in a spherical, unilamellar vesicle in a bulk dispersion on the other hand is difficult with the spectroscopic and scattering techniques available for the characterization of colloidal dispersions. The average tilt angle is related to the birefringence of the bilayers in vesicles and to the linear dichroism of absorption bands.

It has been attempted to access β in vesicles through depolarized light scattering studies [21]. Later, based on the spherical symmetry of vesicles, it was argued that the the depolarized light scattering intensity from spherical vesicles with a radially birefringent shell vanishes [22]. For the analysis of classical static light scattering experiments, modeling lipid vesicles (up to ∼50 nm radius) as isotropic hollow spheres in the Rayleigh-Debye-Gans approximation has been shown to be sufficient [23]. Therefore, a technique which is based on the measurement of transmitted light trough crossed polarizers was established by Mishima and coworkers to access the birefringence of vesicles [24–26]. In most experiments, a quantity proportional to the birefringence of the vesicles is determined and the effects of insertion of e. g. cholesterol or lysophospholipids can be studied qualitatively [25,26]. The determination of the magnitude of the average tilt angle is still problematic, though an early work reports results for the birefringence from which an average tilt angle of ∼45° for DPPC in micrometer-sized vesicles can be calculated [24]. The problems for a precise determination of the vesicle birefringence arise from non-idealities in the optical systems used for the experiments, such as birefringence of cuvettes, entrance and exit windows, non-idealities and misalignment of polarizers, etc. These non-idealities have major contributions to the measured intensities, hence to the obtained birefringence of the vesicles, and are hard to compensate for.

Recently, ellipsometric light scattering (ELS) was established in our lab as a technique that applies the principles of ellipsometry to scattered light [27,28]. The sensitivity of the technique to layers on colloidal particles has been demonstrated. The ellipsometric principle has several advantages over simple transmission measurements. Above all, with the application of zone averaging, many of the mentioned non-idealities cancel in first order, and the remaining birefringence contributions can be determined accurately [29]. In this work, we describe the application of ELS to determine the birefringence of unilamellar lipid vesicles of ∼50 nm radius at 25 °C. Differences between 1,2-Dipalmitoyl-*sn*-glycero-3-phosphocholine (DPPC) in the gel–phase and 1,2-Dioleoyl-*sn*-glycero-3-phosphocholine (DOPC) in the liquid–crystalline phase are found and discussed.

For DPPC, a lower limit of the average tilt angle is derived from the measured birefringence.

2 Experiments

2.1 Vesicle preparation

DPPC and DOPC were purchased from Avanti (Alabaster, USA) in chloroform solution. The chloroform was evaporated in an air stream. After vacuum pumping for 2 h, the respective lipid was dispersed in deionised water through vortexing several times for half a minute to give a 1 g/L dispersion. Subsequently, unilamellar vesicles were prepared in stages using a pneumatic extruder (Avestin Inc., Ottawa, Canada). Firstly, the lipid dispersion was pushed 41 times through a track-etched membrane (Avanti) with a pore radius of 100 nm. In a second stage, the dispersion was extruded 51 times through membrane with 50 nm pore radius. In the case of DPPC all extrusions were performed at 50°C after a five minute equilibration time to ensure the solution is heated above the main phase transition temperature. DOPC was extruded at room temperature. This type of extrusion procedure has been used by many labs and has been shown to yield almost exclusively unilamellar vesicles [30]. For the scattering experiments, the dispersions were diluted to a concentration of 0.1 g/L.

2.2 Ellipsometric light scattering

The details of the method and the setup have been described elsewhere [27]. Briefly, polarizer, compensator and analyzer (Bernhard Halle, Berlin, Germany) as in a null-ellipsometer were built into a light-scattering goniometer setup (ALV, Langen, Germany). The ellipsometric technique then allows for the determination of the ratio

$$\frac{S_2}{S_1} = \tan(\Psi) \cdot \mathrm{e}^{i\Delta} \tag{1}$$

of the diagonal elements of the amplitude scattering matrix [29,31],

$$\begin{pmatrix} E_H \\ E_V \end{pmatrix}^{(f)} = \frac{\exp\left(ik(r-z)\right)}{-ikr} \begin{pmatrix} S_2 & 0 \\ 0 & S_1 \end{pmatrix} \cdot \begin{pmatrix} E_H \\ E_V \end{pmatrix}^{(i)}. \tag{2}$$

Here, $k = 2\pi n_{\mathrm{med}}/\lambda$ is the wave vector modulus for light of vacuum wavelength λ within the medium of refractive index n_{med}, z is the position of the scattering particle along the beam, r is its distance to the detector. The polarization of scattered and incident light are denoted by $\binom{E_H}{E_V}^{(f)}$ and $\binom{E_H}{E_V}^{(i)}$, respectively. E_V is the electric field component polarized perpendicular to the scattering plane, and E_H the component within the scattering plane. The diagonal form of the scattering matrix is valid for particles with spherical symmetry. Beside isotropic spherical particles, this also includes spherical particles with radial birefringence [32].

By applying two-zone averaging, most of the imperfections of the optical system are compensated for [27,29]. For samples with slightly varying particle geometry, it is useful to consider the coherent and the incoherent part of the scattering signal separately, in analogy to a similar distinction in neutron scattering [33]. While the coherent part represents the averaged scattering properties of the particles, the incoherent part stems from deviations from the average for individual particles. The coherent scatter-

ing has a well defined, in general elliptical polarization and therefore can be completely extinguished in the applied nulling ellipsometry. In contrast, the light polarization is completely lost for the incoherent part, which does not affect the nulling ellipsometry measurement. As a consequence, only the coherent part determines the data of a nulling ellipsometry experiment. A favorable aspect of this principle for slightly polydisperse samples has been briefly addressed in reference [28].

As in reflection ellipsometry, the parameters $\tan(\Psi)$ and Δ are particularly sensitive to the properties of the coating of a spherical particle around the angle where $\tan(\Psi)$ is at minimum. In analogy to the terminology in reflection measurements this angle is addressed as Brewster angle Θ_B [27,29]. For ELS on particles smaller than λ, Θ_B is found to be around a scattering angle Θ of 90°. The angular alignment of the experimental setup was checked with isotropic poly(styrene) particles, which yield a minimum of $\tan(\Psi)$ at the value expected for isotropic particles [28].

2.3 Refractive index and refractive index increments

The refractive index of bulk water at $\lambda = 633$ nm has been measured on an Abbe refractometer type 60/ED (Bellingham + Stanley, England). The refractometer was illuminated via an optical fiber by the light of a HeNe Laser (PL-3000, Polytec, Berlin, Germany). The refractive index increments of DPPC and DOPC were measured using a Scanref interferometer (NFT, Göttingen, Germany).

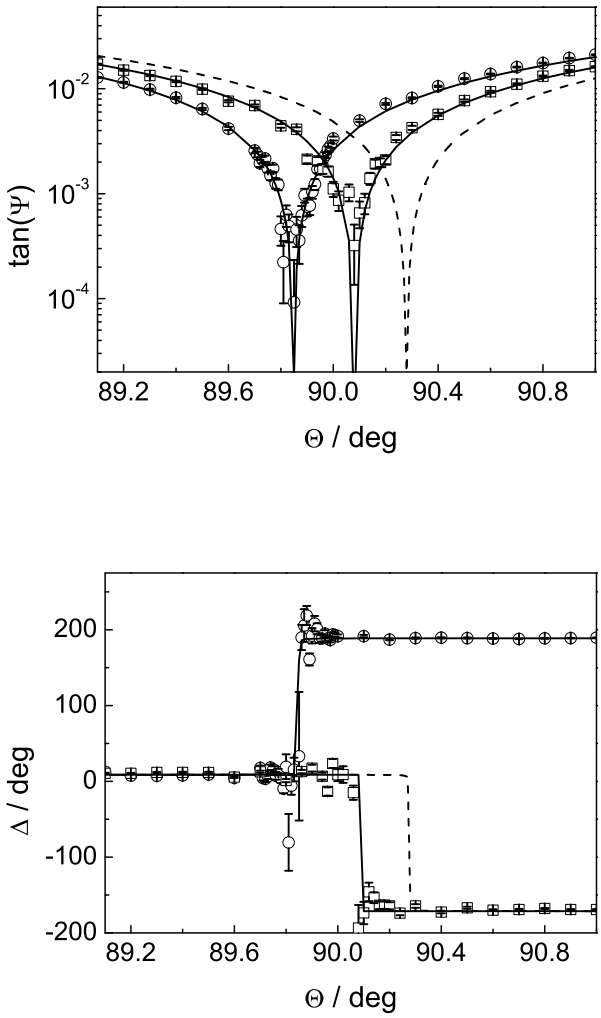

Fig. 1. Ellipsometric parameters $\tan(\Psi)$ and Δ of the respective vesicles at 25 °C. Circles (◯) represent the measured data for DPPC, squares (□) the data for DOPC. The dotted lines are the results as expected for a hollow sphere with an isotropic shell ($R_{\mathrm{tot}} = 45$ nm, $d_s = 5$ nm, $n_s = 1.475$). Continuous lines are the fits to a model based on Mie theory of a radially birefringent shell.

3 Results

Fig. 1 shows the ellipsometric parameters $\tan(\Psi)$ and Δ of unilamellar vesicles of DPPC and DOPC at 25 °C.

In both cases, the total radius R_{tot} of a vesicle is assumed to equal the hydrodynamic radius (DPPC: $R_h = (45 \pm 1)$ nm, DOPC: $R_h = (44 \pm 1)$ nm), determined by angle-dependent dynamic light scattering. The thickness d_s of the lipid bilayer is known from many experiments and found to be in the range of $d \simeq 5$ nm [34]. The refractive index of DPPC vesicles has been determined as a function of temperature by Yi and MacDonald [35]. Extrapolating their data to 25 °C yields $n_s \sim 1.475$, which will be used for further analysis throughout this work. This value is consistent with results found for other lipids [36–39]. To check the refractive index, we have determined the refractive index increment $\mathrm{d}n/\mathrm{d}c$ of DPPC as 0.138 mL/g. With the DPPC density of 1.06 g/mL [34], $n_s \sim 1.478$ is obtained. For DOPC, the same value $n_s \sim 1.478$ follows from $\mathrm{d}n/\mathrm{d}c = 0.146$ mL/g using a density of 1.00 g/mL [34]. The refractive index n_{med} of the surrounding medium water at 633 nm has been determined as $n_{\mathrm{med}} = 1.3317$.

As a first attempt to explain the obtained data, the aforementioned parameters were used to simulate $\tan(\Psi)$ and Δ for a shell with an isotropic coating. The measured data are far away from the results of these simulations, represented as dotted line in Fig. 1. While for DPPC in the experiment the minimum in $\tan(\Psi)$ is at a scattering angle lower than 90°, Mie theory [31,40] of a vesicle with isotropic shell predict the minimum to be located significantly above $\Theta = 90°$. For isotropic layers, a Brewster angle below $\Theta = 90°$ corresponds to negative contrast, i. e. $n_s < n_{\mathrm{med}}$.

The effect of radial birefringence on light scattered by spherical shells was first calculated by Roth and Dignam [32]. They derived expressions for S_1 and S_2 for a coated sphere. As opposed to the isotropic coating, in their model the coating is uniaxially birefringent. For light with the electric field vector tangential and normal to the local interface (TE and TM mode, respectively), the relevant components of the dielectric tensor are n_t^2 and n_n^2, respectively. Here, n_t and n_n are the corresponding refractive indexes. The theory by Roth and Dignam has subsequently been corrected by other authors [41]. An expansion for small values of shell thickness divided by vesicle radius [42] shows deviations from the exact solution, particularly around Θ_B. Therefore, the exact solution was incorporated into the fitting function. The complete set of equations used for the fits is listed in the appendix of this work. The two refractive indexes were parameterized by the birefringence $\Delta n = n_n - n_t$ and the average refractive index $n_{\mathrm{ave}} = \frac{1}{3}n_n + \frac{2}{3}n_t$.

Fits of the results for $\tan(\Psi)$ and Δ to a model based on Roth and Dignam's theory are shown as continuous lines in Fig. 1. The total radius of the vesicles as well as the thickness of the bilayer were fixed at the known values described above. For DPPC, the average refractive index is kept fixed at $n_{\mathrm{ave}} = 1.475$, as mentioned above. The only adjustable parameter is therefore the birefringence Δn of the vesicle's shell. As a result of the fit, $\Delta n = 0.077 \pm 0.001$ is obtained for DPPC. This value is in good agreement with the birefringence obtained from near-field scanning optical microscopy (NSOM) experiments [45]. For DOPC

with a refractive index of 1.478, the obtained birefringence is much lower, $\Delta n = 0.038 \pm 0.001$.

In order to ensure the validity of these results, the effect of changes in the fixed parameters d_s, $R_{\rm tot}$ and $n_{\rm ave}$ have been studied. A change in the layer thickness d_s has almost no effect on the resulting Δn: changing d_s from 5 to 4 nm changes the result by ∼1 %. This finding is not surprising, since the birefringence in a layer with $d_s \ll \lambda$ induces only a minor phase difference between TE and TM mode. The observed strong effect of Δn enters through the boundary conditions at the layer interfaces, and these boundary conditions are independent of layer thickness. The low sensitivity to the actual layer thickness implies that the difference in the layer thickness between DOPC and DPPC is negligible for the analysis. Changing $R_{\rm tot}$ by 10% yields a ∼5% change in Δn, showing a slightly bigger effect. Since $R_{\rm tot}$ is known from independent dynamic light scattering measurements, this is no additional complication. There is a large effect of changes in $n_{\rm ave}$ on Δn. An accurate value for the average refractive index has a crucial impact on the validity of the results. From calculations on isotropic spherical particles it is known that increasing $R_{\rm tot}$ or $n_{\rm ave}$ results in a larger positive shift of Θ_B from $\Theta = 90°$. In the fitting of the present anisotropic vesicles, such a positive shift is compensated by a higher value of Δn, in order to match the position of Θ_B defined by the data.

4 Discussion

4.1 The Average Chain Tilt Angle

DPPC is in the gel–phase at 25 °C, and its acyl chains are in an all–*trans* conformation [34]. For an estimation of β for DPPC, we follow the same reasoning as Aragón and Pecora [22]. For a uniaxially birefringent phase, the orientational order parameter S can be obtained from Δn as

$$S = \frac{p_{ave}}{\Delta p} \frac{2 n_{\rm ave} \Delta n}{n_{\rm ave}^2 - 1}, \qquad (3)$$

with the anisotropy of the polarizability $\Delta p = p_{||} - p_{\perp}$ and the average polarizability $p_{ave} = \frac{1}{3} p_{||} + \frac{2}{3} p_{\perp}$ [22,43]. The polarizabilities parallel ($p_{||}$) and perpendicular ($p_{\perp}$) to the hydrocarbon chain are known for CH_2 groups. Here, the values $p_{||} = 2.14 \cdot 10^{-30}$ m^3 and $p_{\perp} = 1.61 \cdot 10^{-30}$ m^3 have been used [22]. From these polarizabilities, the experimentally determined values of Δn and $n_{\rm ave} = 1.475$, one obtains $S = (0.65 \pm 0.01)$. In a microscopic approach, S is related to the tilt angle β_j of the individual chain j

$$S = \frac{3 \left\langle \cos^2 \beta_j \right\rangle_j - 1}{2}, \qquad (4)$$

where $\langle . \rangle_j$ denotes the ensemble average over all chains.

The interpretation of S needs to be discussed in more detail. Especially the involved averaging process needs a closer inspection. Locally, the tilt of neighbouring chains is correlated and domains with constant tilt direction are formed. Due to the correlation of tilting directions, the molecular order parameter S_m calculated by an equation similar to eq. 4 with the local director as axis of symmetry is expected to be close to 1.

On the length scale of an entire vesicle, one may need to consider the average of the tilt directions over different domains. For planar bilayers, the domain size is known. The correlation lengths obtained from X-ray scattering [18,34,44] or the domain size detected in NSOM experiments [45] exceeds the diameter of the vesicles investigated here. On small spherical vesicles, however, the domain size might be considerably smaller. A smooth orientational field is not possible on a closed spherical manifold for topological reasons. As a consequence of the Gauss-Bonet theorem, singularities breaking the spherical symmetry of vesicles are inevitable [46]. In addition, the bilayer curvature induces a local decrease in S_m. This implies a reduction of the relevant liquid crystalline elastic constants [47], which determine the domain size.

An ELSexperiment averages on an even larger length scale: there is a multitude of vesicles with different orientations of the tilt directions present in the scattering volume. Therefore, the measured value of S is an ensemble average of possible orientational fields on a vesicle. For perfect local molecular order ($S_m = 1$), S describes the distribution of director orientations around a radial direction. For $S_m < 1$, S contains both, the effects of molecular order within a domain as well as the distribution of director orientations.

For a first estimation β_0 for the true average β, the width of the orientation distribution function for the averaging in eq. 4 is neglected, which implies $\left\langle \cos^2 \beta_i \right\rangle_i = \cos^2 \beta_0$. Based on this approximation, the inversion of eq. 4 yields $\beta_0 = (29 \pm 0.5)^\circ$ from the experimental value of S. A refinement starts from the assumption of a narrow distribution around the average tilt angle β. The deviations $\Delta\beta_i = \beta - \beta_i$ are small. With an expansion of $\cos^2(\beta + \Delta\beta_i)$ to second order in $\Delta\beta_i$, the averaging yields $\left\langle \cos^2(\beta + \Delta\beta_i) \right\rangle_i = \cos^2 \beta + \cos(2\beta) \left\langle \Delta\beta_i^2 \right\rangle \geq \cos^2 \beta$. The inequality holds for $\beta \leq 45^\circ$ and implies β_0 to be a lower limit for the average tilt angle. The limiting value is comparable with the chain tilt angle $\beta_{\mathrm{planar}} = 32^\circ$ in planar bilayers [34]. There is only a minor effect of the curvature, as long as only the average tilt angle is considered.

A detailed molecular description of the chain conformation within the bilayer is possible [48], though it requires many assumptions. Packing arguments in a simpler coarse-grained picture can already be used to derive the average chain tilt angle and the layer anisotropy. This approach predicts the tilt angle to significantly decrease in the outer monolayer and to increase in the the inner monolayer. The results obtained here for DPPC suggest that these two opposing influences cancel each other, because the obtained value of β is very similar to the value obtained for planar bilayers.

As opposed to DPPC, the DOPC molecule contains unsaturated hydrocarbon chains which cannot adopt an all–trans conformation. At room temperature, DOPC is therefore in the liquid–crystalline phase. Consequently, the birefringence is significantly reduced compared to DPPC. Calculating S in the same manner as outlined above yields $S = (0.32 \pm 0.01)$. For simplicity, the polarizabilities of the methylene groups have been used here. Because of the presence of one double bond within each DOPC chain, the

true polarization anisotropy is slightly larger and the result for S is slightly overestimated. The finite value of S differs from an isotropic situation ($S = 0$), because the bilayer structure and the geometric constraints imposed by the headgroup packing force the outer segments of the hydrocarbon chain to be partially oriented. This result is consistent with literature data for other lipids in the liquid–crystalline phase, where infrared spectroscopy [49–51] and optical birefringence [26] measurements find a non-vanishing anisotropy.

4.2 Light Scattering of Vesicles with Correlated Tilt Directions

The occurrence of domains of different tilting directions breaks the spherical symmetry of individual vesicles. Despite this broken symmetry, the experimental results are well described by the simple model of spherically symmetric birefringent particles. This finding can be understood by analyzing the magnitude of the different contributions to the ELS signals. ELS detects the coherent scattering contribution (see section 2.2). This averaged scattering from all particles is the ensemble average described above. In the data evaluation in section 3, the averaged scattering of the ensemble was approximated by the scattering of a particle with averaged properties: the ensemble averaged dielectric tensor of the bilayers of vesicles with different tilt directions has an uniaxial form in spherical coordinates. A quantitative theoretical analysis of the quality of this approximation, which will be referred to as the "average particle approximation", requires (not available) detailed information of the orientation field of the tilt directions in each vesicle, and a corresponding description of the Mie scattering properties of such a vesicle.

A similar "average particle approximation" can be applied to and quantitatively tested on polydisperse samples. It turns out that the approximation works well if the form factor of the particles has a small curvature. The vesicles investigated here are small compared to the wavelength of light, therefore showing only a minor curvature in the form factor. Furthermore, the magnitude of the error of the "average particle approximation" is comparable to the tiny magnitude of the incoherent scattering contribution, since both are based on the same non-idealities.

Because of the broken symmetry in individual vesicles, there is no longer a symmetry argument for the absence of depolarized light scattering. However, the effect is very weak. The singularities in the orientational fields of the tilt directions do not imply the presence of singularities of the local birefringence. In the experiments here, the depolarized (VH) scattering intensity was found to be less than 1/2000 of the polarized (VV) intensity. A quantitative evaluation of depolarized light scattering would require a detailed calibration of other sources of polarization loss, like multiple scattering and effects of stress birefringence of the optical windows in the experiment. Since these effects are not considered, the true VH intensity originating from the sample is considerably lower than the measured intensity. Consequently, depolarized light scattering does not affect ELS measurements. Contributions of similar tiny magnitude are expected for the coherent

scattering, making deviations from the "average particle approximation" difficult to detect.

5 Conclusions

Ellipsometric light scattering experiments on phospholipid vesicles with a birefringent shell show the surprisingly high sensitivity of the method to anisotropy. Although the layer thickness is less than 1 % of the wavelength of light, there is a significant shift of the Brewster angle. The magnitude of this shift has been utilized to determine the tilt angle β of the acyl chains in small unilamellar DPPC vesicles with bent bilayers. Based on a theory of Mie scattering for particles with a spherical symmetric birefringence [32,41], a lower limit of $(29 \pm 0.5)^\circ$ is established for β. This result is comparable to the literature value $\beta = (32 \pm 0.5)^\circ$ for oriented planar multi-bilayers [17,34]. Vesicles of DOPC show a much lower birefringence, as expected for vesicles in the liquid–crystalline phase.

The sensitivity of ellipsometric light scattering to local anisotropy opens up the possibility to study other colloidal systems with radial birefringence, e. g. liquid crystals at colloidal interfaces in dispersion. Further potential applications to lipid vesicles with added biological membrane constituents can easily be thought off.

We thank Jeremy Pencer and Antje Reinecke for their help with vesicle extrusion, and Birgit Schonert for the dn/dc measurements. Kerstin Wagner and Stefan Wellert are acknowledged for initially drawing our attention to important references. We are indebted to Markus Antonietti for his steady support. Financial support of the Max Planck Society is gratefully acknowledged.

6 Appendix – Mie theory for a birefringent sphere with radial birefringence

The general principles of Mie theory and equations for the calculation of S_1 and S_2 for a sphere with isotropic coating can be found in the book of Kerker [40]. Kerker's treatment was extended to coatings with radial birefringence by Roth and Dignam [32], whose formulations were later corrected by the group of Aragón [41,42]. In this appendix, the corrected equations needed are compiled in a compact form. The matrix elements S_1 and S_2 follow from representing the incident plane wave as a superposition of spherical waves as

$$S_1 = \sum_{l=1}^{\infty} \frac{2l+1}{l(l+1)} \left[a_l \frac{P_l^{(1)}(\cos\Theta)}{\sin\Theta} + b_l \frac{dP_l^{(1)}(\cos\Theta)}{d\Theta} \right]$$
$$S_2 = \sum_{l=1}^{\infty} \frac{2l+1}{l(l+1)} \left[b_l \frac{P_l^{(1)}(\cos\Theta)}{\sin\Theta} + a_l \frac{dP_l^{(1)}(\cos\Theta)}{d\Theta} \right], \tag{5}$$

where Θ is the scattering angle and $P_l^{(1)}$ are associated Legendre polynomials. The Mie coefficients a_l and b_l are given as

$$a_l = \frac{[\psi\psi]^e_{l,\alpha}\,[\chi\psi]^e_{l,\nu} - [\chi\psi]^e_{l,\alpha}\,[\psi\psi]^e_{l,\nu}}{[\psi\psi]^e_{l,\alpha}\,[\chi\zeta]^e_{l,\nu} - [\chi\psi]^e_{l,\alpha}\,[\psi\zeta]^e_{l,\nu}} \tag{6}$$

and

$$b_l = \frac{[\psi\psi]^m_{l,\alpha}\,[\chi\psi]^m_{l,\nu} - [\chi\psi]^m_{l,\alpha}\,[\psi\psi]^m_{l,\nu}}{[\psi\psi]^m_{l,\alpha}\,[\chi\zeta]^m_{l,\nu} - [\chi\psi]^m_{l,\alpha}\,[\psi\zeta]^m_{l,\nu}}. \tag{7}$$

Here, the operator–like expressions are given as

$$[\chi\psi]^e_{l,\alpha} = m_1{}^e \chi_l'(m_t\alpha)^m \psi_l(m_1\alpha) -$$

$$m_t\,{}^e\chi_l(m_t\alpha)\,{}^m\psi_l'(m_1\alpha), \tag{8}$$

$$[\chi\psi]^e_{l,\nu} = {}^e\chi_l'(m_t\nu)\,{}^m\psi_l(\nu) - m_t\,{}^e\chi_l(m_t\nu)\,{}^m\psi_l'(\nu), \tag{9}$$

$$[\chi\psi]^m_{l,\alpha} = m_t\,{}^m\chi_l'(m_t\alpha)\,{}^m\psi_l(m_1\alpha) - m_1\,{}^m\chi_l(m_t\alpha)\,{}^m\psi_l'(m_1\alpha), \tag{10}$$

$$[\chi\psi]^m_{l,\nu} = m_t\,{}^m\chi_l'(m_t\nu)\,{}^m\psi_l(\nu) - {}^m\chi_l(m_t\nu)\,{}^m\psi_l'(\nu), \tag{11}$$

and the analogous equations for $[\psi\psi]^e_{l,\alpha}$, etc.

The Ricatti-Bessel functions ${}^\mu\psi_l(kr)$, ${}^\mu\chi_l(kr)$, and ${}^\mu\zeta_l(kr)$ are defined as [52]

$${}^\mu\psi_l(kr) = \left(\frac{\pi}{2}kr\right)^{\frac{1}{2}} J_w(kr), \tag{12}$$

$${}^\mu\chi_l(kr) = -\left(\frac{\pi}{2}kr\right)^{\frac{1}{2}} Y_w(kr), \text{ and} \tag{13}$$

$${}^\mu\zeta_l(kr) = {}^\mu\psi_l(kr) - i\,{}^\mu\chi_l(kr). \tag{14}$$

Here, the order w of the Bessel functions $J_w(kr)$ and $Y_w(kr)$ depends on the mode μ, which is either transverse–electric (m) or transverse–magnetic (e). If $\mu = e$,

$$w = \left(l^2(\frac{m_t}{m_n})^2 + l(\frac{m_t}{m_n})^2 + \frac{1}{4}\right)^{\frac{1}{2}} - \frac{1}{2}, \tag{15}$$

while for $\mu = m$,

$$w = l. \tag{16}$$

The relative refractive indices m_t, m_n and m_1 are defined as

$$m_t = n_t/n_{\text{med}}, \tag{17}$$

$$m_n = n_n/n_{\text{med}}, \tag{18}$$

$$m_1 = m_c/n_{\text{med}}, \tag{19}$$

and the size parameters as

$$\alpha = \frac{2\pi n_{\text{med}}(R_{\text{tot}} - d)}{\lambda}, \text{ and} \tag{20}$$

$$\nu = \frac{2\pi n_{\text{med}} R_{\text{tot}}}{\lambda}. \tag{21}$$

Here, m_c is the complex refractive index of the core of the coated sphere. For the case of vesicles with the same medium on the inside as on the outside, $m_c = n_{\text{med}}$ and therefore, $m_1 = 1$.

References

1. A. Janshoff, C. Steinem, Anal. Bioanal. Chem. **385**, 433 (2006).
2. A. Leitmannova Liu (editor), *Advances in Planar Lipid Bilayers and Liposomes. Vol. 3* (Academic Press, Amsterdam 2006). A. Ottova-Leitmannova, H.T. Tien (editors), *Planar lipid bilayers (BLMs) and their applications* (Elsevier, Amsterdam 2003).
3. N. Düzgünes (editor), *Liposomes. Part A-F.* (Elsevier, Amsterdam 2003-2005).
4. R. Maget-Dana, Biochim. Biophys. Acta **1462**, 109 (1999).
5. H. Möhwald, Annu. Rev. Phys. Chem. **41**, 441 (1990).
6. L.J.C. Jeuken, S.D. Connell, P.J.F. Henderson, R.B. Gennis, S.D. Evans, R.J. Bushby, J. Am. Chem. Soc. **128**, 1711 (2006).
7. G. Valincius, D. J. McGillivray, W. Febo-Ayala, D.J. Vanderah, J.J. Kasianowicz, M. Lösche, J. Phys. Chem. B **110**, 10213 (2006).
8. P. Booth, R. Templer, W. Meijberg, S. Allen, A. Curran, M. Lorch, Crit. Rev. Biochem. Mol. Biol. **36**, 501 (2001).
9. A.P. Girard-Egrot, S. Godoy, L.J. Blum, Adv. Colloid Interface Sci. **116**, 205 (2005).
10. P. Dynarowicz-Łątka, A. Dhanabalan, O.N. Oliveira Jr., Adv. Colloid Interface Sci. **91**, 221 (2001).
11. Y.F. Dufrêne, G.U. Lee, Biochim. Biophys. Acta **1509**, 14 (2000).

12. J.B. Peng, G.T. Barnes, I.R. Gentle, Adv. Colloid Interface Sci. **91**, 163 (2001).
13. C.D. Bain, P.R. Greene, Curr. Opin. Colloid Interface Sci. **6**, 313 (2001).
14. J.H. van Zanten, in *Vesicles*, edited by Morton Rosoff (Marcel Dekker, New York 1996).
15. W. Hübner, H.H. Mantsch, Biophys. J. **59**, 1261 (1991).
16. D. Vaknin, K. Kjaer, J. Als-Nielsen, M. Lösche, Biophys. J. **59**, 1325 (1991).
17. S. Tristram-Nagle, R. Zhang, R.M. Suter, C.R. Worthington, W.-J. Sun, J.F. Nagle, Biophys. J. **64**, 1097 (1993).
18. W.-J. Sun, R. M. Suter, M. A. Knewtson, C. R. Worthington, S. Tristram-Nagle, R. Zhang, J.F. Nagle, Phys. Rev. E **49**, 4665 (1994).
19. X. Bin, S.L. Horswell, J. Lipkowski, Biophys. J. **89**, 592 (2005).
20. E. Maltseva, A. Kerth, A. Blume, H. Möhwald, G. Brezesinski, ChemBioChem **6**, 1817 (2005).
21. K. Mishima, J. Colloid Interface Sci. **73**, 448 (1980).
22. S.R. Aragón, R. Pecora, J. Colloid Interface Sci. **89**, 170 (1982).
23. J.H. van Zanten, H.G. Monbouquette, J. Colloid Interface Sci. **165**, 512 (1994).
24. K. Mishima, K. Satoh, T. Ogihara, Biochim. Biophys. Acta **898**, 231 (1987).
25. K. Mishima, K. Satoh, K. Suzuki, Colloids Surf. B **7**, 83 (1996).
26. K. Mishima, K. Satoh, K. Suzuki, Colloids Surf. B **33**, 185 (2004).
27. A. Erbe, K. Tauer, R. Sigel, Phys. Rev. E **73**, 031406 (2006).
28. A. Erbe, K. Tauer, R. Sigel, Langmuir **23**, 452 (2007).
29. R.M.A. Azzam, N.M. Bashara *Ellipsometry and Polarized Light* (Elsevier, Amsterdam 1977).
30. R.C. MacDonald, R.I. MacDonald, B.Ph.M. Menco, K. Takeshita, N.K. Subbarao, L.-R. Hu, Biochim. Biophys. Acta **1061**, 297 (1991).
31. C.F. Bohren, D.R. Huffman *Absorption and Scattering of Light by Small Particles* (John Wiley, New York 1983).
32. J. Roth, M.J. Dignam, J. Opt. Soc. Am. **63**, 308 (1973); J. Roth, M.J. Dignam, J. Opt. Soc. Am. **66**, 981 (1976).
33. J. S. Higgins, H. C. Benoît *Polymers and Neutron Scattering* (Clarendon, Oxford 1996).
34. J.F. Nagle, S. Tristram-Nagle, Biochim. Biophys. Acta **1469**, 159 (2000).
35. P.N. Yi, R.C. MacDonald, Chem. Phys. Lipids **11**, 114 (1973).
36. D. Den Engelsen, Surface Sci. **56**, 272 (1976).
37. D. Ducharme, J.-J. Max, C. Salesse, R.M. Leblanc, J. Phys. Chem. **94**, 1925 (1990).
38. M. Thoma, M. Schwendler, H. Baltes, C.A. Helm, T. Pfohl, H. Riegler, H. Möhwald, Langmuir **12**, 1722 (1996).
39. Z. Salamon, G. Tollin, Biophys. J. **80**, 1557 (2001).
40. M. Kerker *The Scattering of Light and Other Electromagnetic Radiation* (Academic Press, San Diego 1969).
41. B. Lange, S.R. Aragón, J. Chem. Phys. **92**, 4643 (1990).
42. D.K. Hahn, S.R. Aragón, J. Chem. Phys. **101**, 8409 (1994).
43. D.A. Dunmur, in *The Optics of Thermotropic Liquid Crystals*, edited by S. Elston and R. Samles (Taylor & Francis, London 1998), pp. 5-40.
44. K.Y.C. Lee, A. Gopal, A. von Nahmen, J.A. Zasadzinski, J. Majewski, G.S. Smith, P.B. Howes, K. Kjaer, J. Chem. Phys. **116**, 774 (2002).

45. C.-W. Lee, R. S. Decca, S. R. Wassall, J. J. Breen, Phys. Rev. E **67**, 061914 (2003).

46. F. David, in: D. Nelson, T. Piran, S. Weinberg (editors) *Statistical Mechanics of Membranes and Surfaces*, (World Scientific, Singapore 2004).

47. P. G. de Gennes, J. Prost *The Physics of Liquid Crystals*, 2nd edition (Clarendon, Oxford 2003).

48. N. Kučerka, J.F. Nagle, S.E. Feller, P. Balgavý, Phys. Rev. E **69**, 051903 (2004).

49. S. Frey, L.K. Tamm, Biophys. J. **60**, 922 (1991).

50. P. Wenzl, M. Fringeli, J. Goette, U.P. Fringeli, Langmuir 10, 4253 (1994).

51. Y. Cheng, N. Boden, R.J. Bushby, S. Clarkson, S.D. Evans, P.F. Knowles, A. Marsh, R.E. Miles, Langmuir **14**, 839 (1998).

52. M. Abramowitz, I.A. Stegun (editors) *Handbook of mathematical functions*, (Dover, New York 1965).